Universal probes for antiferromagnetic correlations and entropy in cold fermions on optical lattices

E. V. Gorelik,[1] D. Rost,[1] T. Paiva,[2] R. Scalettar,[3] A. Klümper,[4] and N. Blümer[1]

[1] *Institute of Physics, Johannes Gutenberg University, Mainz, Germany*
[2] *Instituto de Fisica, Universidade Federal do Rio de Janeiro, Brazil*
[3] *Department of Physics, UC Davis, USA*
[4] *University of Wuppertal, Wuppertal, Germany*

(Dated: December 20, 2011)

We compute short-range properties of the half-filled Hubbard model at strong coupling using determinantal quantum Monte Carlo (DQMC) and within dynamical mean-field theory for the cubic lattice as well as for the square lattice and Hubbard chain using DQMC and Bethe ansatz. When parametrized by entropy, as is appropriate in the cold-atom context, these observables are surprisingly insensitive to dimensionality and long-range order. In particular, the entrance into the regime of local antiferromagnetism (AF) is signaled by a universal minimum of the double occupancy at entropy $s \approx \log(2)$ and the onset of next-nearest neighbor spin correlations below. Thus, unique AF signatures are (almost) within reach of cold-atom experiments with current cooling techniques. [Comparisons with the Heisenberg model and the weak-coupling case are included.] [The weak coupling case appears not suitable for experimental studies due to the lower critical entropies and less pronounced AF signatures.]

PACS numbers: 67.85.-d, 03.75.Ss, 71.10.Fd, 75.10.-b

A thorough understanding of materials with strong electronic correlations is not only desirable on intellectual grounds, but also due to their increasing technological importance, e.g., in magnetoresistive and superconducting devices [1, 2]. Theoretical investigations of corresponding Hubbard type models have already shed light on many strong-coupling phenomena including metal-insulator transitions, heavy-fermion and non-Fermi-liquid behavior, and various types of magnetic and orbital order [3]. However, there are still important open questions, most notably regarding high-temperature superconductivity, for which so far no mechanism could conclusively be established. Recently, a novel class of correlated Fermi systems, namely ultracold fermionic atoms (such as ^{40}K and ^{6}Li) on optical lattices, has opened a new promising direction of research: cold atoms are predicted to serve as *quantum simulators* for the Hubbard type solid-state Hamiltonians of interest [4–6].

Indeed, the recent experimental observation and quantitative theoretical analysis of the signatures in the compressibility [8] and in the integrated double occupancy [9] has proved the Mott metal-insulator transition in two-flavor mixtures of ^{40}K on cubic optical lattices. As a result, it is now established that the single-band Hubbard model

$$\hat{H} = -t \sum_{\langle ij \rangle, \sigma} \hat{c}^{\dagger}_{i\sigma} \hat{c}_{j\sigma} + U \sum_{i} \hat{n}_{i\uparrow} \hat{n}_{i\downarrow} \qquad (1)$$

(with hopping amplitude t, onsite interaction U, and $\hat{n}_{i\sigma} = \hat{c}^{\dagger}_{i\sigma} \hat{c}_{i\sigma}$) can be realized to a reasonable accuracy using ultracold fermions in the interesting interaction range, which certainly supports the hopes of accessing also less understood Hubbard physics in similar ways.

However, all attempts of realizing and detecting *quantum magnetism* in cold lattice fermions have failed so far. In fact, it has not even been possible yet to verify specific signatures of antiferromagnetic (AF) correlations which are ubiquitous in correlated electrons and believed to play an important role in high-temperature superconductivity. This type of physics clearly has to be under control before cold fermions can really play a useful role as *quantum simulators*. Up to now the failures to detect AF signals have primarily been attributed to cooling issues [10, 11]. Indeed, the coldest systems achieved so far have central entropies per particle of $s \equiv S/(Nk_B) \approx \log(2) \approx 0.69$ [12] while AF long-range order (LRO) on a cubic lattice is expected only for entropies $s < s_{\mathrm{N}} \approx 0.34$ [11, 13, 14]. Moreover, the concept of LRO is not rigorously defined and might be misleading in the finite and inhomogeneous systems realized in fermionic experiments, with a shortest experimental length scale of about 10 lattice spacings [18]. In contrast, short-range correlations remain well-defined. Therefore, experimentalists should focus (initially) on establishing *local* AF; this is possible, as we will show, via signatures in the local observables, i.e. double occupancy D or next-nearest neighbor spin correlations: such measurements can not only quantify nearest-neighbor AF correlations, but also define the regime where a spin picture (i.e., the quantum Heisenberg model) is applicable.

[Motivation? Broader overview!!]

Our calculations in the strong-coupling regime of the half-filled Hubbard model using DMFT, determinantal QMC, and Bethe ansatz reveal AF signatures in the double occupancy D, spin correlations, and kinetic energy already at $s \lesssim \log(2)$, i.e. in experimental reach

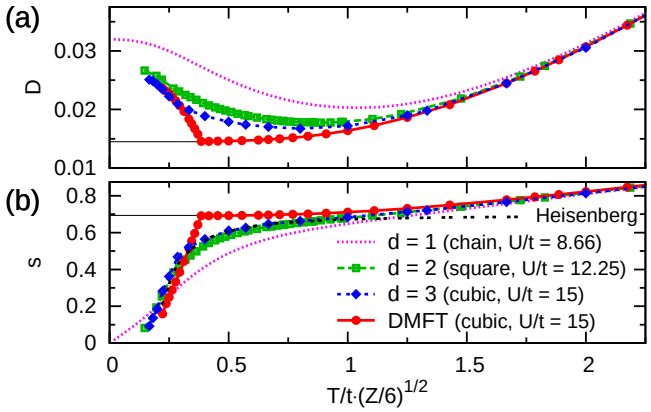

FIG. 1. (Color online) Hypercubic lattice ($1 \le d \le 3$) at strong coupling $U/(\sqrt{Z}t) \approx 6$: a) Double occupancy $D(T)$ as estimated from DMFT ($d = 3$, circles), DQMC ($d = 3$: diamonds, $d = 3$: squares), and BA ($d = 1$, dotted line). b) Corresponding estimates of entropy per particle $s = S/(Nk_{\rm B})$.

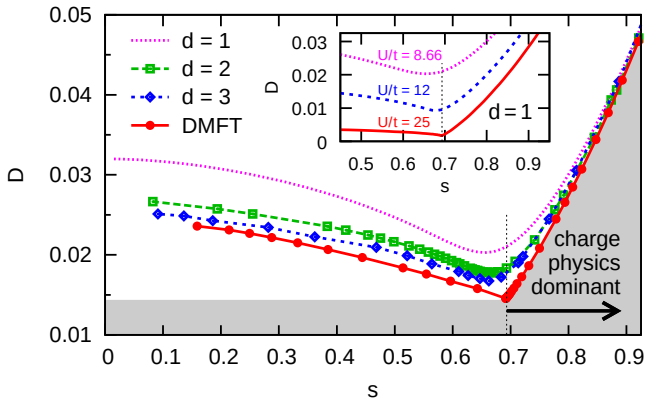

FIG. 2. (Color online) Hypercubic lattice at strong coupling: Double occupancy versus entropy. In all cases, the minimum of the double occupancy corresponds to $s \approx \log(2)$ (dotted line). The shaded area indicates the nonmagnetic contribution to D. Inset: $D(s)$ in $d = 1$ for various interactions.

[12], with surprising universality regarding dimensionality, when viewed as a function of entropy (which is appropriate in the cold-atom context). Both the onset of next-nearest neighbor spin correlations and a minimum in the double occupancy clearly separate the AF Heisenberg regime (at $s \lesssim \log(2)$) from dominant charge physics and should be used experimentally to probe both the AF correlations and the entropy of the system.

AF signatures in the double occupancy and the impact of dimensionality – Signatures in D have previously been linked to antiferromagnetism within dynamical mean-field theory (DMFT). According to DMFT, the low-temperature formation of an AF core in a fermionic cloud on an optical lattice (with central filling $n = 1$) is signaled, at strong coupling, by a distinct enhancement of D in the same region. The absolute increase of D is largest for $U/t \approx 12$; it should be detectable even in experiments integrating over the whole cloud [20]. It is, however, clear that not all aspects of the DMFT scenario are realistic: after all, DMFT overestimates the Néel temperature by up to 30% in the simple cubic case [29, 30]. Thus, sharp signatures in $D(T)$ (cf. Fig. 1a) cannot remain at $T_{\rm N}^{\rm DMFT}$ (except for the weak-coupling regime $U/t \lesssim 6$). But what is, precisely, the impact of finite dimensionality?

In order to gain more insight into these issues, DMFT and QMC data for the cubic lattice are compared at $U/t = 15$ with QMC results for the square lattice and BA solutions of the infinite chain at equivalent [33] interactions in Fig. 1a. Here, the DMFT data (circles) can also be interpreted as an exact result in infinite dimensions. After rescaling [33], we find rapid convergence with increasing dimensionality at high T and generally similar shapes of $D(T)$ for $1 \le d \le \infty$. Still, $d \gg 3$ would apparently be needed in order to converge to the DMFT results also at $T_{\rm N}^{\rm DMFT}$. Furthermore, the minimum in $D(T)$ occurs at or above twice $T_{\rm N}^{\rm DMFT}$ in dimensions $1 \le d \le 3$.

On the other hand, not temperature T, but the entropy s is the experimentally relevant control parameter. Fig. 1b shows numerically exact data for $s(T)$, obtained directly for $d = 1$, and via the thermodynamic relation (valid for $n = 1$)

$$S(\beta) = \log(4) + \beta E(\beta) - \int_0^\beta d\beta' E(\beta')$$

(with $\beta = 1/(k_B T)$ and energy E) for $d = 2, 3$ and DMFT. The agreement between $d = 2$ and $d = 3$ is striking; the latter results converge to the Heisenberg limit for $T \lesssim 0.8t$. Remarkably, the AF DMFT solution (circles for $T < T_{\rm N}^{\rm DMFT}$) recovers the QMC results for the cubic lattice (diamonds) at $T \lesssim T_{\rm N} \approx 0.25t$. This shows that the previously criticized [23] saturation of nonmagnetic solutions (dotted line) at $\log(2)$ for $T \to 0$ is an artifact of the phase restriction, not of DMFT itself.[too much?]

In Fig. 2 we present the experimentally relevant curves $D(s)$, obtained by combining the data of both panels of Fig. 1. While the overall general agreement between the data sets and the regular dimensional convergence at both high and low s already appear striking, our study reveals an important physical fact not realized so far: the minimum in D (at strong coupling) corresponds to $s \approx \log(2) = s_{\rm N}^{\rm DMFT}$ in all dimensions, down to $d = 1$. *A posteriori,* this behavior is easy to understand: $s < \log(2)$ is only possible for a two-flavor system at $n = 1$ by spin coherence, i.e. the development of (possibly short ranged) AF correlations; these, in turn, enhance D [20]. A practical consequence of our finding is that, contrary to earlier expectation, cooling to $s < \log(2)$ will give experimental access to AF physics in any dimension at strong coupling; $s < \log(2)/2$ is not needed.

More generally, the evolution of D is a near-perfect thermometer for ultracold atoms measuring AF corre-

lations and (in $d = 3$) the proximity to AF LRO. In fact, any positive deviation of $D(s)$ from the nonmagnetic background (shaded in Fig. 2) should be linked to AF correlations, generalizing Takahashi's ground state expression [19]

$$D_0 = \frac{Zt^2}{2U^2}\left(1 - \langle \hat{\boldsymbol{\sigma}}_i \cdot \hat{\boldsymbol{\sigma}}_j \rangle_0\right) + \mathcal{O}\left(\frac{t^4}{U^4}\right). \qquad (2)$$

Here, $\langle \hat{\boldsymbol{\sigma}}_i \cdot \hat{\boldsymbol{\sigma}}_j \rangle_0$ is the nearest-neighbor correlation in the quantum Heisenberg model (at $T = 0$): $\langle \hat{\boldsymbol{\sigma}}_i \cdot \hat{\boldsymbol{\sigma}}_j \rangle_0 = -1.00$ ($d = \infty$, Weiss MF); -1.20 ($d = 3$) [34]; -1.34 ($d = 2$) [35, 36]; -1.77 ($d = 1$) [19], which is stronger in lower d, consistent with our finite-T results. Thus, irrespective of the measurement technique, signatures of AF correlations may be easier to detect experimentally (at fixed s) for lower (effective) dimensionality. Conversely, a tuning of the hopping amplitude in z direction could help to discriminate magnetic effects from those of charge excitations; similar ideas including frustration will be explored in a separate publication [37].

Although going beyond the strong coupling regime may, from the first sight, seem favourable due to the higher values of D, it does not bring any real advantages. The AF features are less pronounced in double occupancy, as well as in other local observables (i.e. in totel or kinetic energy, spin correlations). Moreover, decreasing the onsite interaction beyond $U/(\sqrt{Z}t) \lesssim 4$ reduce the critical entropy.

AF signatures in other observables – As we just demonstrated above, in the strong coupling regime the onset of local antiferromagnetism is signaled by the minimum in double occupancy at $s \approx s_{\rm N}^{\rm DMFT} = \log(2)$. Corresponding signatures appear also in other local observables. So, the kinetic energy E_{kin} in $d = 1$ exhibit shoulder at $s \approx s_{\rm N}^{\rm DMFT}$, which transforms into the maximum with increasing the dimensionality, see Fig. 3a. The total energy $E = E_{kin} + UD$ being a monotonous function of entropy shows a kink in this entropy interval. Neither the total energy, nor its kinetic and potential components reveal any visible signature at the Néel phase transition $s_{\rm N} = \log(2)/2$ in $d = 3$. Although this could be attributed to the finite-size effects or numerical noise in DQMC calculations, the main begetter here is the entropy representation. Indeed, it is easy to show that peaks in specific heat, as appear due to the phase transitions, are heavily suppressed and smoothed when energy is considered as a function of entropy. Our "local probes for local order" conclusion is also supported by the recent experimental observation, that even as a function of temperature local properties are unaffected by magnetic phase transition [42].

Spin correlation functions, and especially the one between the nearest neighbors (NN), are probably the most discussed observables in the context of experimental detection of AF in lattice fermions [11, 15, 16, 41]. The NN spin correlation function appears also as a natural choice

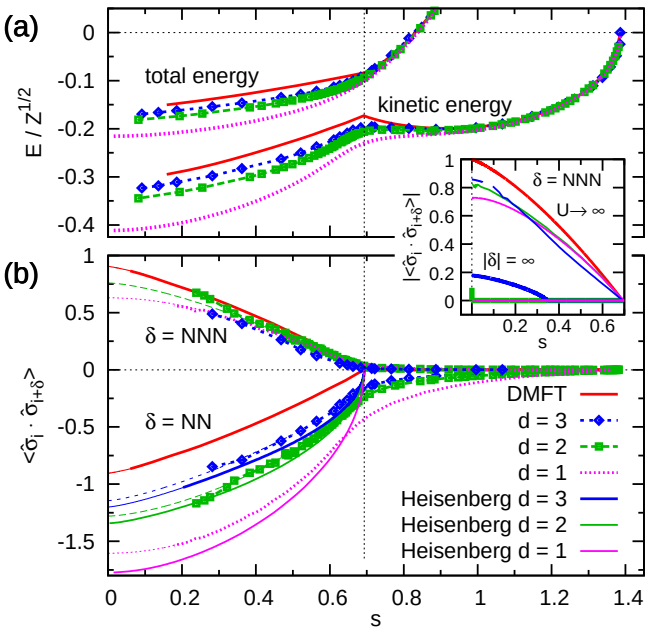

FIG. 3. (Color online) Hypercubic lattice at strong coupling: a) Rescaled total and kinetic energy versus entropy. b) Spin correlations $\langle S_i \cdot S_{i+\delta} \rangle$ between nearest neighbours [$\delta_{d=1} = 1$, $\delta_{d=2} = (1,0)$, $\delta_{d=3} = (1,0,0)$)] and between next-nearest neighbours [$\delta_{d=1} = 2$, $\delta_{d=2} = (1,1)$, $\delta_{d=3} = (1,1,0)$]. Inset: next-nearest neighbours and infinite-range spin correlations for the Heisenberg model.

from the perspective of the Heisenberg model, describing the relevant spin physics in the strong coupling limit. However, if the onsite interaction is strong-but-finite, NN spin correlation function possess strong high-entropy tails for all finite dimensions d, see Fig. 3b. It does not provide any specific signal, neither by the onset of local spin order at $s_{\rm N}^{\rm DMFT} = \log(2)$ nor at the Néel critical entropy in three dimensions $s_{\rm N} = \log(2)/2$. Therefore it is rather of minor usefullness as an experimental observable to monitor the onset of AF.

It is clear, that the only explicit indication of AF LRO may come from the infinite-range spin correlations, as shown on the inset of Fig. 3 (for the Heisenberg model). However, the experimental relevance of this signal and of the LRO itself is not obvious on the length scale of the experimentally realized systems. And even in the best case, the decrease of the central entropy per particle by factor of 3 to 4 respective to the current state-of-art will be recuired for a detectable signal in $d = 3$, lower dimensions will give no signal at all.

The opposite dimensional tendencies in these two limiting cases (NN vs. LRO) forced us to look in detail into the "intermediate" range. And indeed, already the spin correlations between the next-nearest neighbors (NNN) provide the perfect signal of the local AF: with the dimesion-independent onset at $s \approx s_{\rm N}^{\rm DMFT}$ and the absence of high-entropy tails. The entropy dependence of

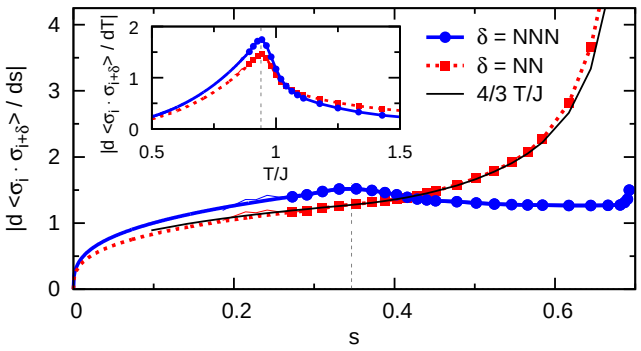

FIG. 4. (Color online) First entropy (main panel) and temperature (inset) derivative of the NN (squares) and NNN (circles) spin correlation functions of the Heisenberg model in $d = 3$.

NNN spin correlations is shown in Fig. 3b for the Hubbard model at strong coupling $U/(\sqrt{Z}t) \approx 6$, and on the inset of Fig. 3 for Heisenberg model. Going to larger spin-spin distances will (i) further suppress the amplitude of signal, and (ii) shift down the entropy of the signal onset, with both changes being more pronounced for lower dimensions.

The detailed analysis of spin correlations for the Heisenberg model in $d = 3$ illustrates this special role of the NNN spin correlations. The first temperature derivatives of both NN and NNN spin correlations show typical peak behaviour in the vicinity of the Néel phase transition, see the inset of Fig. 4. In the entropy representation the NN correlation function does not show any discernible feature at the Néel transition, even if one looks at the corresponding derivative (squares in the main panel of Fig. 4). In contrast, the derivative of the NNN correlation function shows a nice peak on a nearly flat background (circles in the main panel of Fig. 4).

[1] Y. Tokura, Phys. Today **56**, 50 (2003).
[2] E. Dagotto, Science **309**, 257 (2005).
[3] V. Anisimov and Y. Izyumov, *Electronic Structure of Strongly Correlated Materials*, Springer Series in Solid-State Sciences, Vol. 163 (Springer, Berlin, 2010).
[4] W. Hofstetter, J. I. Cirac, P. Zoller, E. Demler, and M. D. Lukin Phys. Rev. Lett. **89**, 220407 (2002).
[5] D. Jaksch and P. Zoller, Ann. Phys. (NY) **315**, 52 (2005).
[6] T. Esslinger, Ann. Rev. Cond. Matt. Phys. **1**, 129 (2010).
[7] M. Köhl, H. Moritz, Th. Stöferle, K. Günter, and T. Esslinger, Phys. Rev. Lett. **94**, 080403 (2005).
[8] U. Schneider *et al.*, Science **322**, 1520 (2008).
[9] R. Jördens, N. Strohmaier, K. Günter, H. Moritz, and T. Esslinger, Nature **455**, 204 (2008).
[10] M. Colomé-Tatché, C. Klempt, L. Santos, and T. Vekua, arXiv:1009.2606.
[11] D. Greif, L. Tarruell, T. Uehlinger, R. Jördens, and T. Esslinger, Phys. Rev. Lett. **106**, 145302 (2011).
[12] R. Jördens *et al.*, Phys. Rev. Lett. **104**, 180401 (2010).
[13] F. Werner, O. Parcollet, A. Georges, and S. R. Hassan, Phys. Rev. Lett. **95**, 056401 (2005).
[14] S. Wessel, Phys. Rev. B **81**, 052405 (2010).
[15] C. Kollath, A. Iucci, I. P. McCulloch, and T. Giamarchi, Phys. Rev. A **74**, 041604(R) (2006).
[16] S. Trotzky, Yu-Ao Chen, U. Schnorrberger, P. Cheinet, and I. Bloch, Phys. Rev. Lett. **105**, 265303 (2010).
[17] T. Corcovilos, S. Baur, J. Hitchcock, E. Mueller, and R. Hulet, Phys. Rev. A **81**, 013415 (2010).
[18] Current experimental trap geometries ($\sim 10^5$ fermions) imply AF cores smaller than $40 \times 40 \times 20$ lattice sites, i.e. each AF site will "feel" a boundary within 10 sites.
[19] M. Takahashi, J. Phys. C **10**, 1289-7301 (1977).
[20] E. V. Gorelik, I. Titvinidze, W. Hofstetter, M. Snoek, and N. Blümer, Phys. Rev. Lett. **105**, 065301 (2010).
[21] S. Fuchs *et al.*, Phys. Rev. Lett. **106**, 030401 (2011).
[22] T. Maier, M. Jarrell, T. Pruschke, and M. Hettler, Rev. Mod. Phys. **77**, 1027 (2005).
[23] L. De Leo, J. Bernier, C. Kollath, A. Georges, and V. W. Scarola, Phys. Rev. A **83**, 023606 (2011).
[24] J. Hirsch and R. Fye, Phys. Rev. Lett. **56**, 2521 (1986).
[25] R. Blankenbecler, D. J. Scalapino, and R. L. Sugar, Phys. Rev. D **24**, 2278 (1981).
[26] N. Blümer and E. Kalinowski, Physica B **359**, 648 (2005).
[27] N. Blümer, Phys. Rev. B **76**, 205120 (2007).
[28] G. Jüttner, A. Klümper, and J. Suzuki, Nucl. Phys. B **522**, 471 (1998).
[29] P. R. C. Kent, M. Jarrell, T. A. Maier, and Th. Pruschke, Phys. Rev. B **72**, 060411(R) (2005).
[30] R. Staudt, M. Dzierzawa, and A. Muramatsu, Eur. Phys. J. B **17**, 411 (2000).
[31] Th. Paiva, R. Scalettar, M. Randeria, and N. Trivedi, Phys. Rev. Lett. **104**, 066406 (2010).
[32] See Supplemental Material at ... for an analysis of finite-size and Trotter errors.
[33] All scales are set by the root mean square energy $\langle \epsilon^2 \rangle_{U=0}^{1/2} = \sqrt{Z}t$ (for coordination number Z).
[34] J. Oitmaa, C. J. Hamer, and Z. Weihong, Phys. Rev. B **50**, 3877 (1994).
[35] Z. Weihong, J. Oitmaa, and C. J. Hamer, Phys. Rev. B **43**, 8321 (1991).
[36] A. W. Sandvik, Phys. Rev. B **56**, 11678 (1997).
[37] E. V. Gorelik and N. Blümer, in preparation.
[38] M. Snoek, I. Titvinidze, C. Töke, K. Byczuk, and W. Hofstetter, New J. Phys. **10**, 093008 (2008).
[39] R. W. Helmes, T. A. Costi, and A. Rosch, Phys. Rev. Lett. **100**, 056403 (2008).
[40] N. Blümer and E. V. Gorelik, Comp. Phys. Comm. **118**, 115 (2011).
[41] K. G. L. Pedersen, B. M. Andersen, G. M. Bruun, O. F. Syljuåsen, and A. S. Sørensen, Phys. Rev. A **84**, 041603(R) (2011).
[42] M. Pickel, A. B. Schmidt, M. Weinelt, and M. Donath, Phys. Rev. Lett. **104**, 237204 (2010).
[43] D. C. McKay and B. DeMarco, Rep. Prog. Phys. **74**, 054401 (2011).